Geomechanics and Engineering, Vol. 1, No. 3 (2009) 219-239
DOI: http://dx.doi.org/10.12989/gae.2009.1.3.219

Ratio of predicted and observed natural frequency of finite sand stratum

M.T. Prathap Kumar†

G.C.E., Ramanagara, India and UVCE, Bangalore, India

H.N. Ramesh‡ and M.V. Raghavendra Rao‡†

Faculty of Engineering (Civil), UVCE, Bangalore University, Bangalore, India

M.E. Raghunandan‡‡

UVCE, Bangalore, India

(Received April 24, 2009, Accepted August 20, 2009)

Abstract. Vertical vibration tests were conducted using model footings of different size and mass resting on the surface of finite sand layer with different height to width ratios and underlain by either rigid concrete base or natural red-earth base. A comparative study of the ratio of predicted and observed natural frequency ratio of the finite sand stratum was made using the calculated values of equivalent stiffness suggested by Gazetas (1983) and Baidya and Muralikrishna (2001). Comparison of results between model footings resting on finite sand stratum underlain by the rigid concrete base and the natural red-earth base showed that, the presence of a finite base of higher rigidity increases the resonant frequency significantly. With increase in H/B ratio beyond 2.0, the influence of both the rigid concrete and natural red-earth base decreases. Increase in the contact area of the footing increases the resonant frequency of the model footings resting on finite sand stratum underlain by both the types of finite bases. Both the predicted and the observed resonant frequency ratio decreases with increase in force rating and height to width ratio for a given series of model footing.

Keywords: dynamic response; resonant frequency; displacement amplitude; frequency ratio; equivalent stiffness.

1. Introduction

In the case of machine foundations, the resonance condition results in excessive displacement amplitude of the foundation that is detrimental to the supporting structure. Many investigators (Whitman and Richart 1967, Richart *et al.* 1970, Nagendra and Sridharan 1982, Gazetas 1983,

† Assistant Professor, Research Scholar, Corresponding Author, E-mail: mtprathap_63@rediffmail.com
‡ Professor, Ph.D.
‡† Professor, M. Tech.
‡‡ Former PG Student

1991, to name a few) found that the dynamic response of foundations depends on several factors, such as, size and shape of the foundation, depth of embedment, soil profile and its properties, frequency of loading and mode of vibration. In most of the investigations, the soil medium below the foundation has been assumed to be homogeneous elastic half-space. However, in reality, soils are rarely homogeneous. A hard rock can exist at shallow depth and it may also consist of different strata with different properties. Presence of rigid rock or a hard stratum compared to the top layer is one of the most common features that occur in nature. The resonant frequency and the corresponding displacement amplitude are affected by the nonhomogeneity of soil.

Gazetas and Roesset (1979) have presented a solution for the vertical vibration response of a strip footing resting on the surface of elastic soil layer overlying a rock. It was found that the presence of a thin rigid layer increases the resonant frequency and amplitude compared to the half-space values. Kagawa and Kraft (1981) carried out a parametric study in which the soil deposit was idealized as a two-layered system, the bottom layer being treated as a half-space. It was observed that, large amplitude magnification occur in layered soil compared to the half-space solution and resonant frequency for a two layered system is generally lower than that for elastic half-space. Gazetas (1983) suggested an expression for the vertical stiffness of a finite layer underlain by rigid layer, using the values of shear modulus and Poisson's ratio of soil and thickness of the finite stratum. Sridharan *et al.* (1990) conducted block vibration tests on two and three layered system and suggested a method to estimate the equivalent stiffness of a multi-layered system. Baidya and Sridharan (1994) studied the dynamic response of the foundation resting on a stratum underlain by a rigid layer using lumped parameter model and suggested a method to estimate the equivalent stiffness and equivalent damping. Al-Homoud and Al-Maaitah (1996) conducted forced vertical vibration tests using a universal testing machine to study the effect of mass, area, geometry, embedment and saturation on the natural frequency and amplitude of model footings. On the basis of forced vertical vibration tests, it was concluded that the natural frequency increases with decrease in the corresponding amplitude due to increase in embedment depth, degree of saturation and footing base area. Further, increase in the mass of the foundation resulted in the decrease in natural frequency. Baidya and Muralikrishna (2001) studied through experiments, the influence of layering and presence of rigid boundary in the soil on the resonant frequency and peak displacement amplitude by conducting model block vibration tests in vertical mode. The result of the observed natural frequencies was compared with predicted one, which was obtained using equivalent static stiffness. Mandal and Baidya (2004) conducted model block vibration tests on rigid surface footings to study the effect of the presence of rigid layer at any depth within the soil mass on the dynamic response of foundation under vertical mode of vibration. The resonant frequency of the foundation-soil system decreased considerably with increase in thickness of the soil layer above the rigid base and reached almost a constant value at a depth equal to three times the width of the footing. Baidya and Rathi (2004) conducted vertical vibration tests on model footings to determine the dynamic behavior of foundations resting on sand layer underlain by rigid layer. It was observed that the resonant frequency decreased with increase in thickness of the soil layer above the rigid base and it nearly equals the half-space value when the thickness of the layer exceeds three times the width of the footing.

Few researchers have investigated the dynamic response of foundation on nonhomogeneous soil system. Also, literature available to date for studying the effect of size and mass of the foundation on the dynamic response of foundation resting on nonhomogeneous soil system are scanty. It was aimed to investigate experimentally by conducting vertical vibration tests using model footings of

different size and mass resting on the surface of finite sand layer of different height to width ratios (stratum height to footing width, henceforth called as H/B ratio) underlain by rigid concrete base and natural red-earth base. A comparative study of the predicted and observed frequency ratio of the finite sand stratum was made using the calculated values of equivalent stiffness suggested by Gazetas (1983) and Baidya and Muralikrishna (2001). The experimental results presented here in, provides an insight into the theoretical predictions with regard to the effect of size, mass of the footings and influence of rigid base on the dynamic response of the foundation.

2. Experimental program

2.1 Properties of sand used

The sand used in the present investigation was locally available river sand, whose properties was determined and is as described in Table 1. The test beds were prepared using this sand to specified depths representing a finite sand stratum lying over either the rigid base or the more flexible natural red-earth base. The rigid concrete base is used to simulate the presence of a rock stratum occurring in nature, the location of which is represented by different H/B ratio of the finite sand stratum. In order to study the influence of rigidity of the concrete base on the dynamic response of the foundation-soil system, tests were also performed on the same model footings under similar loading conditions but with footings resting on the finite sand stratum underlain by the more flexible natural red-earth base considering the same H/B ratios of the sand stratum. The results were compared for both the cases.

2.2 Test tank

A test tank of plan size having internal dimensions 1.6 m × 1.6 m and of height 1.2 m with vertical sides simulating a test pit, was constructed at the testing site situated near the Geotechnical Engineering Laboratory of the Bangalore University Campus, using solid concrete blocks after removing the top loose soil to a depth of 300 mm in the natural ground formation and compacting the soil at the site so as to minimize the relative displacements below the rigid concrete base. It is

Table 1 Properties of sand used

Sl. No	PARTICULARS		
1	Specific gravity		2.64
2	Grain size analysis	Coarse sand (%)	0.03
		Medium sand (%)	60.8
		Fine sand (%)	37.8
		Silt and clay (%)	1.31
3	Co-efficient of uniformity(Cu)		2.60
4	Coefficient of curvature (Cc)		1.40
5	Maximum Dry Density, $(Y_d)_{max}$ kN/m^3		18.3
	Minimum Dry Density $(Y_d)_{min}$ kN/m^3		14.6

well established that the width of the tank should be more than 3 to 4 times the maximum width of the model footings for static problems. The maximum width of the model footing used is 300 mm and the maximum thickness of the sand layer considered in the present experimental investigation is 900 mm. Based on the maximum size of the model footings used, the size of the test tank was optimized in order to minimize the boundary reflections. This size is expected to be satisfactory for determining natural frequency of a low damped system and from the consideration of a slope of spreading foundation pressure over depth 2 (vertical): 1 (horizontal). A small opening of about 500 mm × 600 mm was made on one side of the test tank to facilitate easy fixing of the flexible shaft connecting the oscillator (source of vibration mounted on the model footing) with the D.C. motor. For tests with model footings resting on dry sand underlain by the rigid concrete base, a concrete base of 300 mm thickness and of M20 grade was cast and cured at the testing site to represent a finite rigid boundary for the overlying sand stratum. Young's modulus of concrete being very high when compared with the overlying sand layer, as well as natural red-earth base, it has been considered as a rigid layer when compared with natural red-earth base and the overlying sand stratum.

For tests with model footings resting on dry sand underlain by the natural red-earth base, the top loose soil to a depth of 300 mm was removed and the soil at the site was compacted to act as a more flexible but a finite base. Subsurface exploration of the soil at the nearby test site using an open test pit excavated to a depth of 1.5 m showed that the site comprised of thick deposit of red-earth. Since the maximum width of the model footing used in the experimental program is 300 mm and considering the depth of pressure bulb to be two times the width of the model footing, the test site can be assumed to consist of homogeneous soil of red-earth in the present investigation. The red-earth deposit at the site consisted of silt (34%) mixed with sand (54%) and clay (12%). The liquid limit, plastic limit and shrinkage limit of the soil at the site was 31%, 25% and 14% respectively.

2.3 Model footings

Two series of reinforced model footings of square shape and of different thickness using M20 grade cement concrete were cast and cured. All the vertical vibration tests on the model footings were carried out using a constant static weight of 3.0 kN, provided by steel plates fixed on top of the model footing, along with the oscillator assembly. The mass of footings were so fabricated that,

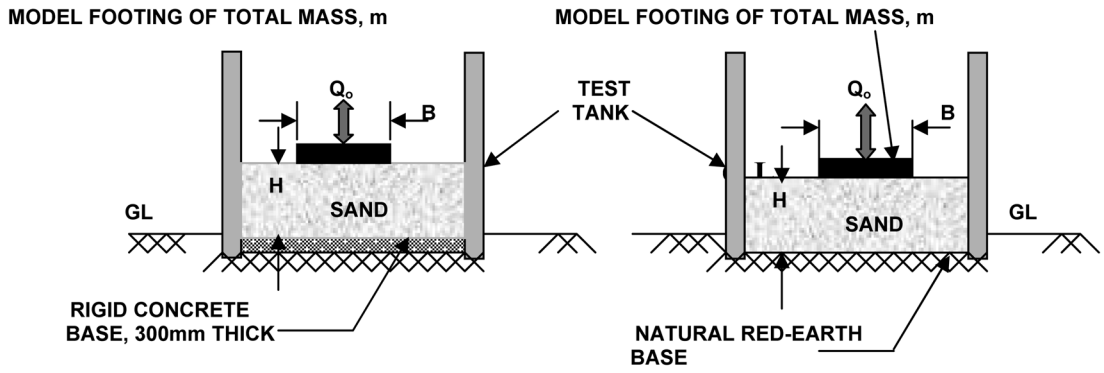

Fig. 1 Schematic diagram of experimental set up

Table 2 Specifications of model footings used

Sl.No.	Series Index	Size of the Model Footing [L×B×H] (mm)	Total Mass of the Model Footing including Oscillator assembly (kN)	Static Weight (kN)	Average Static Pressure at the Base (kN/m^2)
1	SI(A)	200×200×100	1.276		106.9
2	SI(B)	200×200×200	1.408	3.0	110.0
3	SI(C)	200×200×300	1.693		110.8
4	SII(A)	300×300×100	1.431		49.23
5	SII(B)	300×300×200	1.739	3.0	52.66
6	SII(C)	300×300×300	1.861		54.66

each series of model footings along with the constant mass of the oscillator and the static weight of 3.0 kN generated almost equal intensity of static contact pressure at its base when placed over the finite sand stratum, so as to avoid any consequential effects of variation in contact pressure during vibration. Fig. 1 shows the schematic diagram of the experimental set up and Table 2 shows the specifications for the model footings used in the present experimental investigation.

2.4 Preparation of sand layer

Uniformly graded, medium to fine grained, river sand with properties as described in Table 1 was used to prepare test beds of specified thickness to represent a finite sand stratum lying either over the rigid base or the more flexible natural red-earth base. Calculated weight of sand was poured into the test tank in layers of thickness of 100 mm to maintain a uniform condition throughout the test program. Each layer was compacted to maintain uniform density of 17 kN/m^3 so that the desired relative density of 70% was achieved. For compaction, a square steel plate of 400 mm width and 10 mm thickness was placed on sand and was tampered by uniformly distributed 16 blows of a 4.5 kg compaction rammer falling through a height of 457.2 mm. This procedure was used to achieve the required compaction. Several trials were made to know the unit weight γ_d of the sand and the corresponding relative density (D_r) achieved, before starting the test.

2.5 Experimental procedure

After filling sand to the desired thickness, the top surface of the sand bed was leveled and the precast concrete model footing was placed concentrically. The base plate of the oscillator was fixed to the footing by ensuring perfect rigidity of contact between model footing and the oscillator. Mild steel plates were placed on top of the oscillator by suitable arrangement to provide the required static weight of 3.0 kN. The whole setup (model footing, oscillator and steel plates) acts as a single unit, with the center of gravity of whole system and that of the footing to lie in the same vertical line.

The oscillator mounted on the model footing was connected through a flexible shaft to a variable DC motor (5HP capacity, frequency range between 0 to 50 Hz) placed outside the tank. The mechanical oscillator consists of two shafts with eccentric mass mounted on them and so arranged that they rotate in opposite directions at the same speed, when a motor connected through a flexible shaft drives one of them. The rotation of the shaft induces a vertical vibratory force at the base of

the model footing.

A piezoelectric type vibration pickup was placed on top of the footing to measure the displacement amplitude and was connected to 'Data Acquisition System (DAS)' using a low noise cable provided for the purpose. The oscillator was then run slowly by the motor using the speed control unit after setting the desired force rating in the oscillator. The model footings were subjected to vertical mode of vibration at four selected force ratings of 0.016 N-sec^2, 0.024 N-sec^2, 0.032 N-sec^2 and 0.039 N-sec^2. Using the DAS, the frequency in Hertz and the corresponding amplitude of vibration were recorded at regular intervals. Sufficient time gap between two successive measurements was allowed to have a stable reading. Finally the frequency versus amplitude curves was plotted for each of the different tests. Four different force ratings were used in order to simulate different intensities of dynamic excitation. The frequency corresponding to the maximum displacement amplitude was taken as the resonant frequency. Sand was compacted over the natural red-earth base in the same manner and tests were repeated for the same model footings and at the same test conditions.

3. Results and discussions

Four frequency response curves were obtained for each model footing under a static weight of 3.0 kN and for a specified H/B ratio corresponding to four levels of force ratings used. Table 3 and Table 4 show the observed values of resonant frequency and resonant amplitude obtained for both

Table 3 Observed resonant frequency and resonant amplitude of model footings of series SI

Force Ratings (N-sec^2)	Height to Width Ratio (H/B)	Size of the Footing: L×B×H					
		200×200×100 SI(A)		200×200×200 SI(B)		200×200×300 SI(C)	
		f_{nr} Az_{max} (Rigid Concrete Base)	f_{nr} Az_{max} (Natural Red-Earth Base)	f_{nr} Az_{max} (Rigid Concrete Base)	f_{nr} Az_{max} (Natural Red-Earth Base)	f_{nr} Az_{max} (Rigid Concrete Base)	f_{nr} Az_{max} (Natural Red-Earth Base)
0.016	0.0	–	26.8 0.24	–	24.2 0.23	–	22.0 0.20
0.024		–	25.6 0.26	–	23.4 0.25	–	21.2 0.22
0.032		–	24.7 0.29	–	22.1 0.23	–	20.0 0.24
0.039		–	22.4 0.34	–	21.2 0.32	–	19.5 0.28
0.016	0.5	13.5 0.82	11.7 0.78	13.1 0.83	10.8 0.73	12.4 0.75	9.9 0.72
0.024		13.2 0.85	11.3 0.81	12.9 0.85	10.5 0.75	12.2 0.77	9.7 0.74
0.032		12.8 0.93	10.8 0.84	12.7 0.87	10.3 0.77	12.1 0.84	9.3 0.76
0.039		12.4 0.96	10.6 0.88	12.5 0.88	9.8 0.80	11.4 0.87	9.2 0.82

Table 3 Continued

Force Ratings (N-sec^2)	Height to Width Ratio (H/B)	Size of the Footing: L×B×H					
		200×200×100 SI(A)		200×200×200 SI(B)		200×200×300 SI(C)	
		f_{nr} Az_{max} (Rigid Concrete Base)	f_{nr} Az_{max} (Natural Red-Earth Base)	f_{nr} Az_{max} (Rigid Concrete Base)	f_{nr} Az_{max} (Natural Red-Earth Base)	f_{nr} Az_{max} (Rigid Concrete Base)	f_{nr} Az_{max} (Natural Red-Earth Base)
0.016	1.0	10.8 0.65	9.5 0.62	10.4 0.62	9.1 0.60	10.2 0.61	8.2 0.59
0.024		10.6 0.68	8.7 0.64	10.1 0.65	8.6 0.63	9.9 0.64	7.9 0.62
0.032		10.0 0.69	8.3 0.66	9.8 0.66	8.6 0.65	9.2 0.65	7.4 0.64
0.039		9.2 0.71	8.1 0.69	9.6 0.68	8.1 0.68	8.6 0.68	7.1 0.66
0.016	2.0	6.8 0.50	6.6 0.47	6.2 0.48	6.0 0.45	6.0 0.47	5.8 0.46
0.024		6.4 0.51	6.2 0.49	5.9 0.50	5.8 0.48	5.7 0.49	5.6 0.48
0.032		6.2 0.52	6.2 0.51	5.8 0.51	5.5 0.50	5.5 0.51	5.4 0.50
0.039		5.7 0.55	5.9 0.54	5.2 0.53	5.2 0.52	5.1 0.53	5.1 0.52
0.016	3.0	5.9 0.51	5.8 0.48	5.4 0.50	5.2 0.46	5.0 0.47	4.4 0.45
0.024		5.4 0.54	5.2 0.53	4.9 0.51	4.8 0.48	4.8 0.49	4.2 0.47
0.032		4.9 0.55	4.8 0.54	4.5 0.53	4.2 0.514	4.6 0.51	4.2 0.50
0.039		4.5 0.57	4.4 0.55	4.2 0.55	4.1 0.53	4.3 0.53	4.0 0.52

f_{nr}= resonant frequency in Hertz
Az_{max} = Maximum Displacement Amplitude in mm
H/B = 0.0 corresponds to model footings resting directly over natural red-earth base

the series of model footings SI and SII resting on finite sand stratum underlain by both rigid concrete base and natural red-earth base.

3.1 Effect of rigidity and location of the finite base

Fig. 2 shows the variation of the response curve obtained with respect to ratio H/B=0.5 for model footing of series SI (A) with variation in force rating. As seen from Fig. 2, the response curve obtained for model footings resting on finite sand stratum underlain by rigid concrete base has higher value of resonant frequency and the resonant amplitude than those obtained for model footing resting on finite sand stratum underlain by natural red-earth base. Fig. 3 shows the response

Table 4 Observed resonant frequency and resonant amplitude of model footings of series SII

Force Ratings (N-sec^2)	Height to Width Ratio (H/B)	Size of the Footing: L×B×H (in mm)					
		300×300×100 SII(A)		300×300×200 SII(B)		300×300×300 SII(C)	
		f_{nr} Az_{max} (Rigid Concrete Base)	f_{nr} Az_{max} (Natural Red-Earth Base)	f_{nr} Az_{max} (Rigid Concrete Base)	f_{nr} Az_{max} (Natural Red-Earth Base)	f_{nr} Az_{max} (Rigid Concrete Base)	f_{nr} Az_{max} (Natural Red-Earth Base)
0.016	0.0	–	34.0 0.36	–	32.6 0.32	–	28.2 0.21
0.024		–	33.8 0.40	–	30.2 0.35	–	27.4 0.24
0.032		–	32.0 0.44	–	29.0 0.37	–	26.0 0.30
0.039		–	29.6 0.51	–	28.2 0.39	–	25.8 0.34
0.016	0.5	19.0 0.84	13.4 0.78	18.6 0.74	12.5 0.71	14.4 0.70	11.3 0.64
0.024		18.0 0.86	13.0 0.81	17.3 0.75	12.2 0.73	14.0 0.71	11.2 0.68
0.032		16.1 0.87	12.7 0.83	14.5 0.76	11.7 0.75	13.4 0.73	11.1 0.69
0.039		15.2 0.89	12.3 0.88	13.5 0.77	11.4 0.76	12.7 0.75	10.7 0.70
0.016	1.0	13.6 0.79	10.3 0.77	13.4 0.70	8.9 0.66	13.3 0.69	8.2 0.64
0.024		13.2 0.81	9.9 0.79	13.1 0.72	8.5 0.68	13.0 0.74	8.0 0.66
0.032		13.0 0.85	9.3 0.80	12.9 0.74	8.2 0.71	12.8 0.77	7.8 0.72
0.039		12.5 0.88	9.0 0.83	12.2 0.77	7.8 0.74	12.4 0.77	7.5 0.74
0.016	2.0	10.4 0.58	8.6 0.55	9.6 0.56	7.6 0.52	8.0 0.54	7.1 0.52
0.024		9.8 0.60	8.3 0.57	9.5 0.58	7.4 0.56	7.8 0.56	6.8 0.55
0.032		9.4 0.64	7.9 0.62	9.4 0.61	7.2 0.60	7.6 0.58	6.4 0.56
0..039		9.4 0.66	7.5 0.65	9.2 0.64	7.0 0.63	7.4 0.60	6.1 0.59

curve obtained with respect to H/B ratio of 3.0 for model footing of series SI (A) with variation in force rating. As seen from Fig. 3, the difference in response curves obtained for model footing resting on finite sand stratum underlain by both the types of bases are marginal. Same trends have been observed for the entire series of model footings and at all force ratings and H/B ratios used. These variations indicate that the presence of rigid base increases the resonant frequency and the increase is significantly influenced by the rigidity of finite base. Higher the rigidity of the finite base,

Table 4 Continued

Force Ratings (N-sec^2)	Height to Width Ratio (H/B)	Size of the Footing: L×B×H (in mm)					
		300×300×100 SII(A)		300×300×200 SII(B)		300×300×300 SII(C)	
		f_{nr} Az_{max} (Rigid Concrete Base)	f_{nr} Az_{max} (Natural Red-Earth Base)	f_{nr} Az_{max} (Rigid Concrete Base)	f_{nr} Az_{max} (Natural Red-Earth Base)	f_{nr} Az_{max} (Rigid Concrete Base)	f_{nr} Az_{max} (Natural Red-Earth Base)
0.016	3.0	8.6 0.52	6.9 0.50	7.6 0.51	6.1 0.48	6.8 0.50	5.7 0.46
0.024		8.4 0.53	6.3 0.51	7.3 0.55	5.7 0.50	6.4 0.52	5.0 0.49
0.032		8.2 0.55	6.1 0.53	7.1 0.56	5.3 0.52	6.00 0.54	4.7 0.52
0.039		7.8 0.57	5.7 0.55	6.9 0.58	5.1 0.54	5.7 0.55	4.5 0.53

f_{nr} = Resonant frequency in Hertz
Az_{max} = Maximum Displacement Amplitude in mm
H/B = 0.0 corresponds to model footings resting directly over natural red-earth base

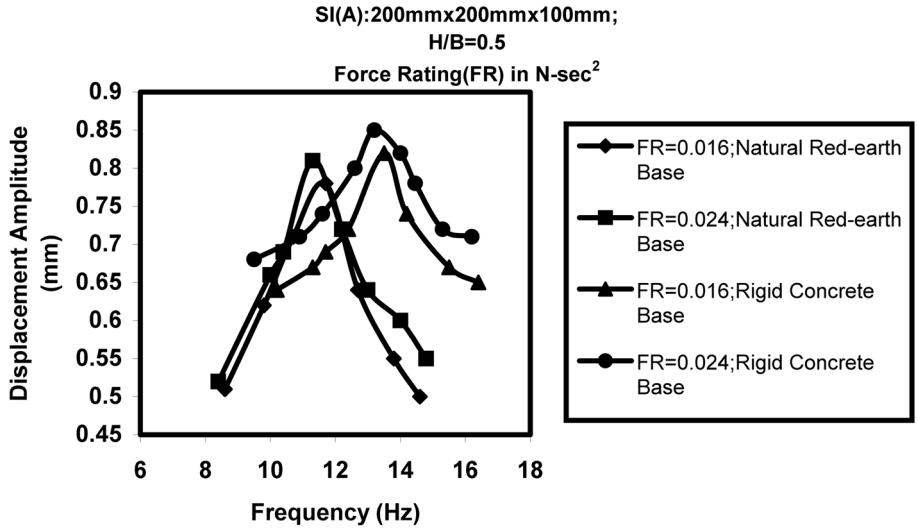

Fig. 2 Variation of response curves of series SI (A) at H/B=0.5

higher will be the resonant frequency. The influence of both the types of base decreases when H/B ratio exceeds 3.0, there by indicating that the finite sand stratum behaves as homogeneous sand stratum.

3.2 Effect of size and mass of the model footings

Fig. 4 and Fig. 5 show comparative variation of resonant frequency with mass ratio, defined as, $b=m/\rho r_o^3$, where, m=total mass of the vibrating footing and oscillator, r_o=equivalent radious of circular contact area=$(A/\pi)^{0.5}$, ρ=mass density of the soil, and A=contact area of the square model

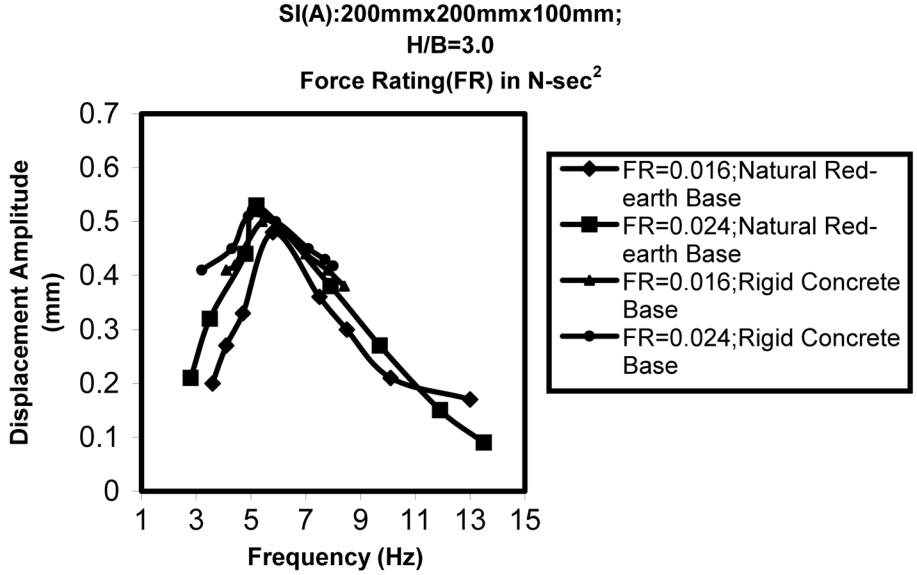

Fig. 3 Variation of response curves of series SI (A) at H/B=3.0

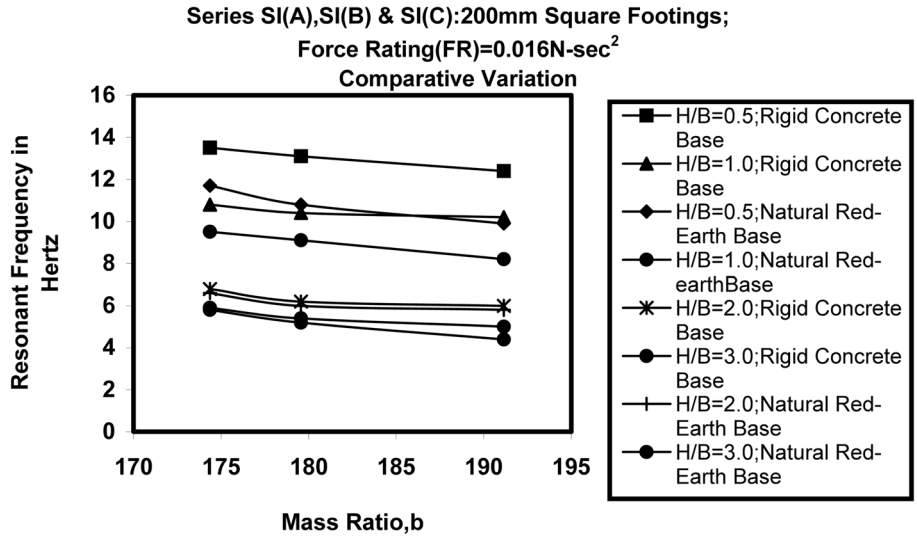

Fig. 4 Comparative variation of resonant frequency with mass ratio of series SI

footing (Reissner 1936)-for model footings of series SI and SII at a force rating of 0.016 N-sec^2. As seen from these Figures, with increase in the mass ratio, the resonant frequency decreases and the decrease is more significant with increase in H/B ratio between 0.5 and 1.0 for both the types of finite base. However, at higher H/B ratios (i.e. beyond H/B=2.0), there is marginal variation in resonant frequency, corresponding to both the types of finite bases at a constant mass ratio of the footing.

Fig. 6 shows the comparative variation of resonant frequency with H/B ratio for model footings of series SI (A) and SII (A), at a constant force rating of 0.016 N-sec^2. As seen from Fig. 6, lower the mass ratio, higher will be the resonant frequency under a constant H/B ratio and at constant force

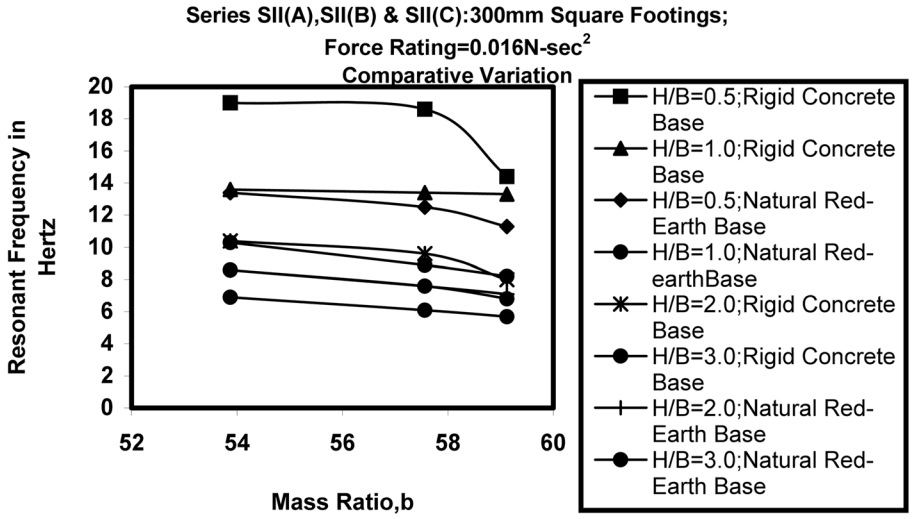

Fig. 5 Comparative variation of resonant frequency with mass ratio of series SII

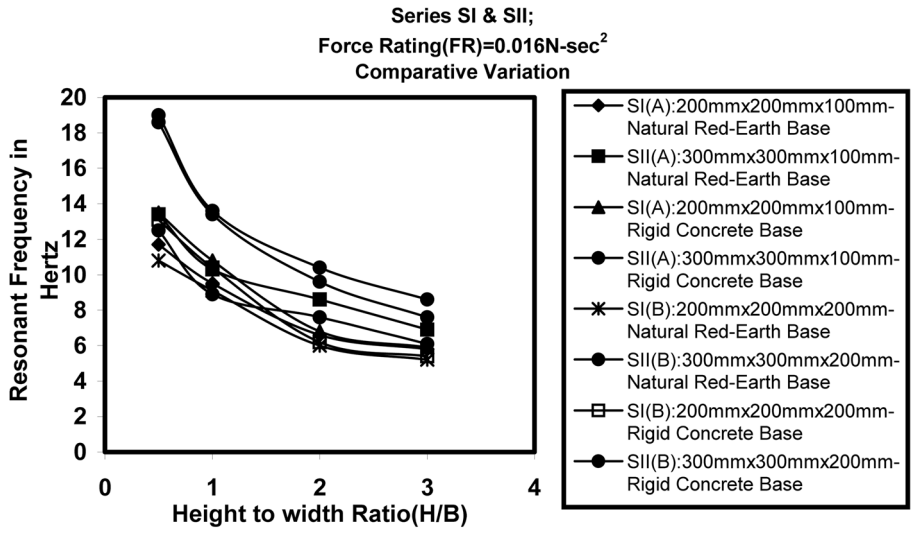

Fig. 6 Comparative variation of resonant frequency with H/B ratio of series SI and SII

rating, for both the types of finite base. At H/B=3.0, for footings with higher mass ratio the value of resonant frequency is almost same with only a marginal variation.

Further, increase in the contact area of the footing decreases the mass ratio of the footing, thereby the resonant frequency of the model footings resting on both the types of finite base increases. This indicates that increase in the area of the footing increases the resonant frequency whereas increase in the mass of the footing for a constant contact area of the footing decreases the resonant frequency. Same trends have been observed at other force ratings used and for the entire series of model footings in the present investigation.

3.3 Predicted and observed frequency ratios

Damping ratio was calculated using the lumped mass-spring dashpot model and using the observed values of resonant frequency obtained for the entire model footings. It was found that the damping ratio for the entire test results was less than 10%. The measured resonant frequency (f_{nr}) is thus taken approximately equal to natural frequency of the foundation-soil system (f_n). The ratio of the natural frequency of a footing resting on a layer of a finite sand stratum f_{nf}, and the one resting on a infinitely homogeneous half-space f_{nh}, can thus be written as:

$$\frac{f_{n_f}}{f_{n_h}} = \frac{\left[\frac{k_f}{m}\right]^{1/2}}{\left[\frac{k_h}{m}\right]^{1/2}} \tag{1}$$

which simplifies to,

$$\frac{f_{n_f}}{f_{n_h}} = \left[\frac{k_f}{k_h}\right]^{1/2} \tag{2}$$

where, k_f = static stiffness of the rigid circular footing resting on a layer of finite thickness underlain by a rigid base,

k_h = static stiffness of the rigid circular footing resting on an infinitely homogeneous half-space, given by,

$$k_h = \frac{4Gr_o}{(1-\mu)} \tag{3}$$

where, G = shear modulus of homogeneous deposit of soil,

r_o = equivalent radius of circular contact area = $(A/\pi)^{0.5}$, and

μ = Poisson's ratio of soil.

It was observed from the present experimental investigation, the influence of finite base at H/B=3.0 are minimum. The value of shear modulus G was computed using measured value of resonant frequency corresponding to the ratio H/B=3.0 for all the series of model footings using the following equation:

$$G = \frac{\omega_n^2(1-\mu)m}{4r_o} \tag{4}$$

where, ω_n = natural frequency of foundation-soil system,

m = total mass of the vibrating system,

r_o = the equivalent radius of the footing, and

μ = Poisson's ratio of soil.

The value of shear modulus thus obtained is used to compute the stiffness of the finite sand stratum resting over rigid concrete base (k_f^* and k_f^{**}) using the Eq. (5) and Eq. (6), suggested by Gazetas (1983) and Baidya and Muralikrishna (2001) respectively, and the stiffness of finite sand stratum over the natural red-earth base (k_f^*) was computed using the Eq. (7) suggested by Gazetas (1983) by considering it as a two layered system as below:

$$k_f^* = \frac{4G_1 r_o\left[1+1.28\frac{r_o}{H}\right]}{(1-\mu)} \tag{5}$$

$$k_f^{**} = \frac{\pi G_1 r_o}{\left|F\right|_0^{\frac{H}{r_o}}} \tag{6a}$$

where, F is a non dimensional depth factor given by,

$$F = \frac{1-\mu}{2}\tan^{-1}\left(\frac{H}{r_o}\right) - \frac{1}{4}\frac{\left(\frac{H}{r_o}\right)}{\left(1+\frac{H^2}{r_o^2}\right)} \tag{6b}$$

Table 5 Ratio of predicted and observed natural frequency f_{fn}/f_{fh} for model footing of series SI at ratio H/B=0.5

Force Rating (N-sec^2)	H/B	SI(A) Predicted Frequency Ratio f_{nf}/f_{nh}* RCB [From Eq.5]	SI(A) Predicted Frequency Ratio f_{nf}/f_{nh}* NRB [From Eq.7]	SI(A) Predicted Frequency Ratio f_{nf}/f_{nh}** RCB [From Eq.6]	Average G (kN/m^2) [Iwasaki *et al.* (1977)]	f_{nh} [Eq.4] (Hertz)	SI(A) Observed Frequency Ratio Observed f_{nf}/f_{nh} RCB	SI(A) Observed Frequency Ratio Observed f_{nf}/f_{nh} NRB
0.016	0.5	1.95	1.85	2.43	52377	4.75	2.84	2.47
0.024		1.78	1.67	2.22			2.78	2.38
0.032		1.61	1.54	2.02			2.69	2.28
0.039		1.48	1.41	1.86			2.61	2.24
		SI(B)				SI(B)		
0.016	0.5	1.81	1.69	2.26	52377	4.67	2.81	2.31
0.024		1.64	1.56	2.05			2.76	2.25
0.032		1.50	1.37	1.88			2.72	2.20
0.039		1.40	1.34	1.76			2.67	2.09
		SI(C)				SI(C)		
0.016	0.5	1.72	1.48	2.16	52377	4.53	2.74	2.19
0.024		1.66	1.41	2.07			2.69	2.14
0.032		1.59	1.40	1.98			2.67	2.06
0.039		1.48	1.34	1.85			2.52	2.03

RCB: For model footings under the Influence of Rigid Concrete Base
NRB: For model footings under the Influence of Natural Red-earth Base
Eq. 5: Gazetas Equation (1983) for finite stratum
Eq.6: Baidya and Muralikrishna (2001) Equation for finite stratum
Eq.7: Gazetas Equation (1983) for two-layered stratum

$$k_f^* = \frac{4G_1 r_o\left[1 + 1.28\frac{r_o}{H}\right]}{(1-\mu_1)\left\{1 + 1.28\left(\frac{G_1}{G_2}\right)\frac{r_o}{H}\right\}} \tag{7}$$

where, k_f^* and k_f^{**} = the vertical equivalent static stiffness of finite stratum,
G_1 = shear modulus of the finite sand stratum,
G_2 = shear modulus of natural red-earth base
H = the thickness of the finite stratum,
r_o = the equivalent radius of the footing, and
μ = Poisson's ratio of soil (taken equal to 0.33 for sand and 0.3 for natural red-earth).

The stiffness of the homogeneous sand deposit (k_h) was evaluated from Eq. (3). The shear modulus of homogeneous deposit of sand was obtained using Eq.(8) suggested by Hardin and Drenvich (1972) and Iwasaki *et al.* (1977) suggestions for constants A and n, which is taken to be equal to 900 and 0.38 respectively.

Table 6 Ratio of predicted and observed natural frequency f_{fn}/f_{fh} for model footing of series SI at ratio H/B=3.0

Force Rating (N-sec^2)	H/B	SI(A) Predicted Frequency Ratio f_{nf}/f_{nh}* RCB [From Eq.5]	SI(A) Predicted Frequency Ratio f_{nf}/f_{nh}* NRB [From Eq.7]	SI(A) Predicted Frequency Ratio f_{nf}/f_{nh}** RCB [From Eq.6]	Average G (kN/m^2) [Iwasaki *et al.* (1977)]	f_{nh} [Eq.4] (Hertz)	SI(A) Observed Frequency Ratio Observed f_{nf}/f_{nh} RCB	SI(A) Observed Frequency Ratio Observed f_{nf}/f_{nh} NRB
0.016	3.0	1.39	1.35	1.75	52377	4.75	1.24	1.22
0.024		1.27	1.21	1.60			1.14	1.09
0.032		1.15	1.12	1.45			1.03	1.01
0.039		1.06	1.03	1.34			0.95	0.93
		SI(B)				SI(B)		
0.016	3.0	1.29	1.23	1.63	52377	4.67	1.14	1.11
0.024		1.17	1.14	1.48			1.03	1.03
0.032		1.07	0.99	1.36			0.95	0.89
0.039		1.00	0.97	1.27			0.88	0.88
		SI(C)				SI(C)		
0.016	3.0	1.23	1.08	1.55	52377	4.53	1.05	0.97
0.024		1.18	1.03	1.49			1.01	0.93
0.032		1.13	1.03	1.43			0.97	0.93
0.039		1.06	0.98	1.34			0.91	0.88

RCB: For model footings under the Influence of Rigid Concrete Base
NRB: For model footings under the Influence of Natural Red-earth Base
Eq. 5: Gazetas Equation (1983) for finite stratum
Eq.6: Baidya and Muralikrishna (2001) Equation for finite stratum
Eq.7: Gazetas Equation (1983) for two-layered stratum

$$G = A\ F(e)\ (P_m)^n \tag{8}$$

where, G = shear modulus,
A & n = constants;
$F(e)$ = constant function of voids ratio
P_m = overburden pressure

Finally, the predicted natural frequency ratio f_{nf}/f_{nh} were computed for different H/B ratios of sand stratum underlain by both the types of finite base.

The observed natural frequency ratio for finite sand stratum underlain by both the rigid concrete base and natural red-earth base was evaluated in the following steps:

The measured values of resonant frequency corresponding to each series of footing at different H/B ratios were considered as f_{nf}. The natural resonant frequency of homogeneous sand stratum (f_{nh}) was obtained by substituting the value of G for homogeneous stratum obtained into Eq. (4). Finally, the observed frequency ratio was evaluated as the ratio of f_{nf}/f_{nh}.

Table 5 and Table 6 show the typical values of the predicted natural frequency ratio $\mathbf{f_{nf}/f_{nh}}$* and observed natural frequency ratio for the model footings of series SI corresponding to H/B ratio of

Table 7 Ratio of predicted and observed natural frequency f_{fn}/f_{fh} for model footing of series SII at ratio H/B=0.5

Force Rating (N-sec^2)	H/B	SII(A)			SII(A)			
		Predicted Frequency Ratio			Observed Frequency Ratio			
		f_{nf}/f_{nh}*		f_{nf}/f_{nh}**	Average G (kN/m^2) [Iwasaki *et al.* (1977)]	f_{nh} [Eq.4] (Hertz)	Observed f_{nf}/f_{nh}	
		RCB [From Eq.5]	NRB [From Eq.7]	RCB [From Eq.6]			RCB	NRB
0.016	0.5	2.21	1.72	2.76	59626	6.00	3.17	2.23
0.024		2.16	1.58	2.70			3.00	2.17
0.032		2.11	1.53	2.63			2.68	2.12
0.039		2.00	1.43	2.51			2.53	2.05
		SII(B)				SII(B)		
0.016	0.5	2.02	1.58	2.52	59626	5.70	3.26	2.19
0.024		1.94	1.63	2.42			3.04	2.14
0.032		1.88	1.38	2.36			2.54	2.05
0.039		1.83	1.33	2.29			2.37	1.99
		SII(C)				SII(C)		
0.016	0.5	1.83	1.50	2.29	59626	5.80	2.48	1.94
0.024		1.72	1.32	2.15			2.41	1.93
0.032		1.61	1.24	2.02			2.31	1.91
0.039		1.53	1.20	1.92			2.19	1.84

RCB: For model footings under the Influence of Rigid Concrete Base
NRB: For model footings under the Influence of Natural Red-earth Base
Eq. 5: Gazetas Equation (1983) for finite stratum
Eq.6: Baidya and Muralikrishna (2001) Equation for finite stratum
Eq.7: Gazetas Equation (1983) for two-layered stratum

Table 8 Ratio of predicted and observed natural frequency f_{fn}/f_{fh} for model footing of series SII at ratio H/B=3.0

Force Rating (N-sec^2)	H/B	SII(A) Predicted Frequency Ratio f_{nf}/f_{nh}* RCB [From Eq.5]	f_{nf}/f_{nh}* NRB [From Eq.7]	f_{nf}/f_{nh}** RCB [From Eq.6]	Average G (kN/m^2) [Iwasaki *et al.* (1977)]	f_{nh} [Eq.4] (Hertz)	SII(A) Observed Frequency Ratio Observed f_{nf}/f_{nh} RCB	NRB
0.016	3.0	1.57	1.26	1.99	59626	6.00	1.43	1.15
0.024		1.54	1.15	1.94			1.40	1.05
0.032		1.50	1.11	1.89			1.37	1.02
0.039		1.43	1.04	1.81			1.30	0.95
		SII(B)					SII(B)	
0.016	3.0	1.44	1.15	1.82	59626	5.70	1.33	1.07
0.024		1.38	1.08	1.75			1.28	1.00
0.032		1.34	1.00	1.69			1.25	0.93
0.039		1.31	0.97	1.65			1.21	0.89
		SII(C)					SII(C)	
0.016	3.0	1.30	1.09	1.65	59626	5.80	1.17	0.98
0.024		1.23	0.96	1.55			1.10	0.86
0.032		1.15	0.90	1.46			1.03	0.81
0.039		1.09	0.87	1.38			0.98	0.78

RCB: For model footings under the Influence of Rigid Concrete Base
NRB: For model footings under the Influence of Natural Red-earth Base
Eq. 5: Gazetas Equation (1983) for finite stratum
Eq.6: Baidya and Muralikrishna (2001) Equation for finite stratum
Eq.7: Gazetas Equation (1983) for two-layered stratum

0.5 and 3.0 respectively and Table 7 and Table 8 show the corresponding values obtained for model footings of series SII. As seen from Tables 5 to 8, for model footings of series SI and SII, the predicted frequency ratio $\mathbf{f_{nf}/f_{nh}}$** obtained using equivalent stiffness as given by Eq. (6)-suggested by Baidya and Muralikrishna (2001) gives larger values of $\mathbf{f_{nf}/f_{nh}}$ when compared with that obtained using equivalent stiffness as given Eq. (5)-suggested by Gazetas's (1983) equation for the case of finite sand stratum underlain by rigid concrete base. Similar trends have been obtained for H/B ratio equal to 1.0 and 2.0.

As seen from Table 6, the predicted frequency ratio at H/B=3.0 and at a force rating of 0.039 N-sec^2 for finite sand stratum underlain by rigid concrete base obtained using Gazetas's Eq. (5) are-1.06, 1.00 and 1.06 for model footings of series SI (A), (B) and (C) respectively whereas the corresponding values for series SII (A), (B) and (C) in Table 8 are-1.43, 1.31 and 1.09 respectively (which has larger contact area when compared to model footings of Series SI). The corresponding values obtained at H/B=3.0 and at a force rating of 0.039 N-sec^2 using Baidya and Muralikrishna's Eq. (6) are 1.34, 1.27 and 1.34 for model footings of series SI (A), (B) and (C) respectively and for series SII (A), (B) and (C) they are equal to 1.81, 1.65 and 1.38 respectively, for the case of finite sand stratum underlain by rigid concrete base. The values at H/B=3.0 indicates the negligible

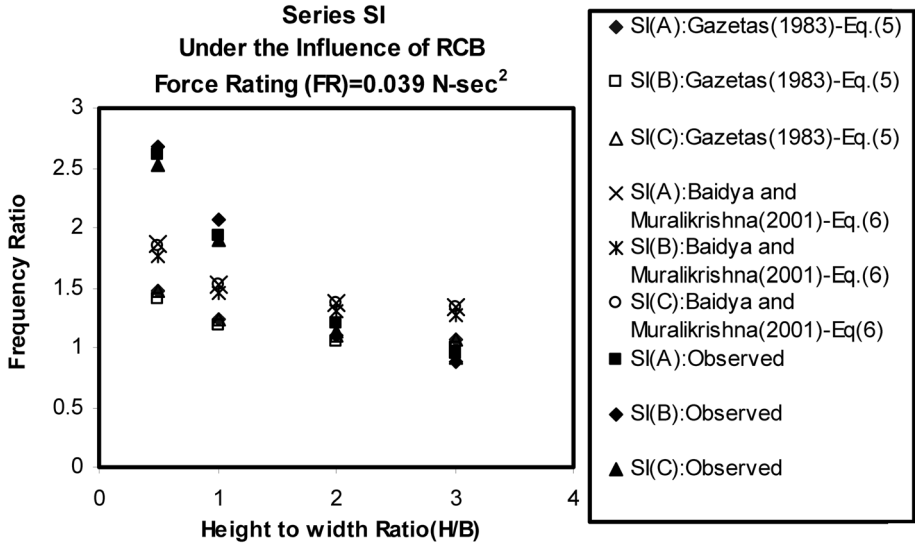

Fig. 7 Ratio of predicted and observed natural frequency of series SI under the influence of rigid concrete base

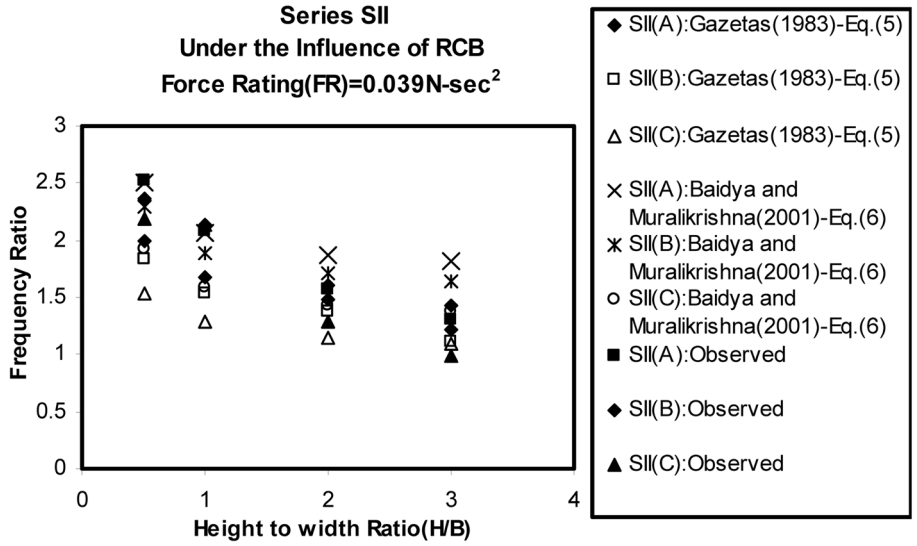

Fig. 8 Ratio of predicted and observed natural frequency of series SII under the influence of rigid concrete base

influence of both the types finite base on the resonant frequency. Same trends have been observed for all the series of model footings and for all the force ratings for the case of finite sand stratum underlain by natural red-earth base.

Figs. 7, 8, 9 and 10 show the variation of predicted and observed natural frequency ratio with variation in H/B ratio for all the series of model footings tested at a force rating of 0.039 N-sec^2. As seen from these figures, both the predicted and observed natural frequency ratios decrease with increase in H/B ratio. The predicted frequency ratio using Baidya and Muralikrishna's (2001)

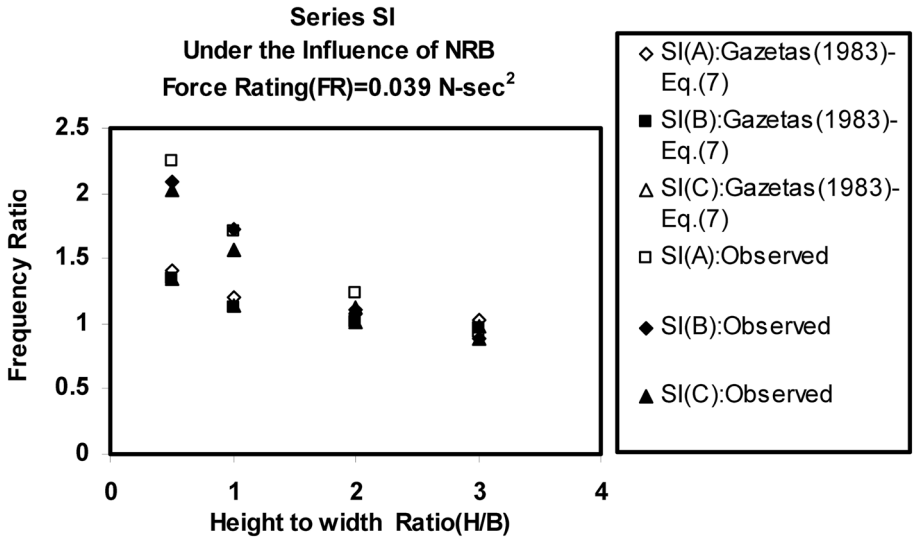

Fig. 9 Ratio of predicted and observed frequency of series SI under the influence of natural red-earth base

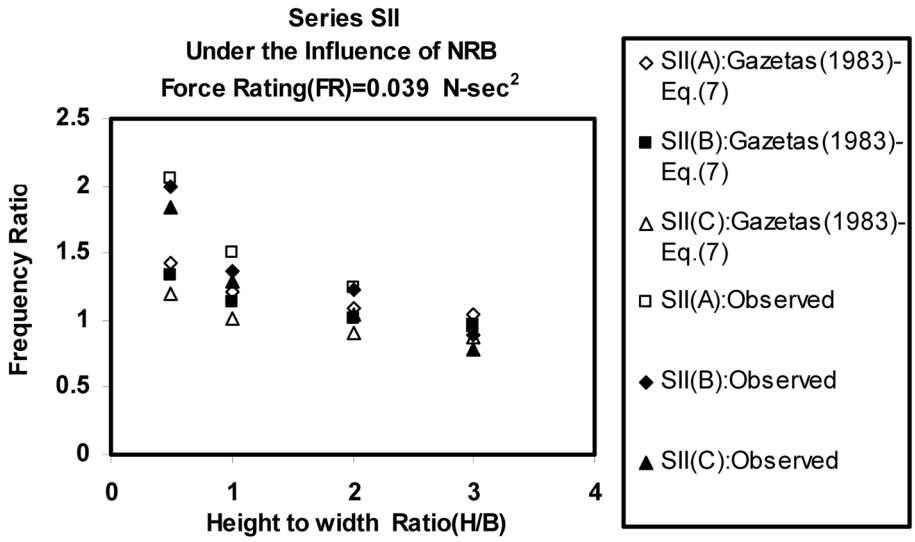

Fig. 10 Ratio of predicted and observed frequency of series SII under the influence of natural red-earth base

equation compares well with observed frequency ratio between ratio H/B=0.5 to 1.0, where as the one computed using Gazetas's (1983) equation compares well with the observed values beyond H/B ratio=2.0 for both the series of model footings. The discrepancy in the experimental results with regard to H/B ratio is due to the certain limitations of the present experimental investigation such as boundaries of the test tank and scale effect of the model footings. The present investigation has been conducted in a tank sufficiently large enough to minimize the boundary effects. However it does not exactly simulate the lateral infinity of the elastic half-space. Further, the pressure bulb formed beneath the model footings is considerably small when compared to the prototype. Hence, most of the soil particles within this pressure bulb can be considered to be in-phase with the

vibrating model footing, which may not be so in actual foundations where in the in-phase soil mass may become insignificant factor. Thus the effect of the boundary of the test tank and the size of the model footings would have contributed to the contradictory results. As seen from Figs. 7, 8, 9 and 10 most of the observed results are in tune with the predicted values and the general trend in both predicted and observed natural frequency ratio is that, both decreases with increase in H/B ratio, which validates the experimental investigation. Further, presence of a base with higher rigidity gives higher values of both the predicted and observed natural frequency ratios. Since the present investigation uses two series of model footing having constant thickness but with increase in area and hence with significant decrease in mass ratio, the trend in the experimental results will be relevant to prototype footings.

4. Conclusions

The results of the experimental study and comparison of results between model footings resting on finite sand stratum underlain by the rigid concrete base and the natural red-earth base showed that:

1. The presence of a finite base of higher rigidity increases the resonant frequency significantly.
2. Location of the finite base and hence the thickness of the finite sand stratum also has significant influence on the resonant frequency of model footings. For example, when the rigid concrete base and natural red-earth base are present at shallow depth, i.e., at H/B=0.5, the measured value of resonant frequency of the model footings were maximum which decreases with increase in H/B ratio.
3. With increase in H/B ratio beyond 2.0, the influence of both the rigid concrete base and natural red-earth base decreases as there is no significant variation in the response curves obtained corresponding to H/B ratio of 3.0.
4. Increase in the contact area of the footing decreases the mass ratio of the footing, thereby the resonant frequency of the model footings resting on finite sand stratum underlain by both the types of finite bases increases. Thus, increase in the area of the footing increases the resonant frequency whereas increase in the mass of the footing for a constant contact area of the footing decreases the resonant frequency. These observations qualitatively agree with theoretical models.
5. Both the predicted and the observed frequency ratio decreases with increase in force rating for a given series of model footing. Also, both the predicted and observed frequency ratios decrease with increase in H/B ratio.
6. The predicted frequency ratio using Baidya and Muralikrishna's (2001) equation compares well with observed frequency ratio between ratio H/B=0.5 to 1.0, where as the one computed using Gazetas's (1983) equation compares well with the observed values beyond H/B ratio =2.0 for both the series of model footings, resting on finite sand stratum underlain by rigid concrete base and natural red-earth base.

References

Al-Homoud, A.S. and Al-Maaitah, O.N. (1996), "An experimental investigation of vertical vibration of model footings on sand", *J. Soil Dyn. Earthq. Eng.*, **15**, 431-445.

Baidya, D.K. and Sridharan, A. (2002), "Foundation Vibration on Layered Soil System", *Indian Geotech. J.*, **32**(2), 236-257.
Baidya, D.K. and Muralikrishna, G. (2001), "Investigation of resonant frequency and amplitude of vibrating footing resting on a layered soil system", *Geotech. Test. J.*, **24**(4), 409-417.
Baidya, D.K. and Rathi, A. (2004), "Dynamic response of footings resting on a sand layer of finite thickness", *J. Geotech. Geoenviron.*, **130**(6), 651-655.
Baidya, D.K., Muralikrishna, G. and Pradhan, P.K. (2006), "Investigation of the foundation vibrations resting on a layered soil system", *J. Geotech. Geoenviron.*, **132**, 116-123.
Gazetas, G. and Rosset, J.M. (1979), "Vertical Vibration of machine foundations", *J. Geotech. Eng. Div.,* ASCE, **105**(12), 1435-1454.
Gazetas, G. (1983), "Analysis of machine foundations: state of the art", *J. Soil Dyn. Earthq. Eng.*, **2**(1), 2-42.
Gazetas, G. (1991), "Formulae and charts for impedances of surface and embedded foundations", *J. Geotech. Eng. Div.*, ASCE, **117**(9), 1363-1381.
Hardin, B.O. and Drenevich, V.P. (1972), "Shear modulus and damping in soils: design equations and curves", *J. Soil Mech. Found. Eng. Div.*, ASCE, **98**(6), 603-624.
Kagawa, T. and Kraft, L.M., Jr. (1981), "Machine foundations on layered soil deposits", *Proceedings of the 10th International Conference on Soil Mechanics and Foundation Engineering*, Stockholm, June.
Lysmer, J. (1965), "Vertical motion of rigid footing", *U.S. Army Engineer Waterways Experiment Station.* Report No.3-115, Vicksburg, Mississippi.
Lysmer, J. and Richart, F.E., Jr. (1966), "Dynamic response of footings to vertical loading", *J. Soil Mech. Found. Eng. Div.,* ASCE, **92**(1), 65-91.
Reissner, E. (1936), "Stationare, axial symmetrische durch eine schuttelnde masse erregate shwingungen eines homogene elastischen halbraums", *Ingeniur-Archiv*, **7**, 681-396.
Mandal, A. and Baidya, D.K. (2004), "Effect of presence of rigid base within the soil on the dynamic response of rigid surface foundation", *Geotech. Test. J.*, **27**(5), 475-482.
Nagendra, M.V. and Sridharan, A. (1982), "Stiffness coefficients of an elastic medium", *J. Geotech. Eng. Div.*, **108**(4), 661-668.
Richart, F.E., Jr, Hall, J.R. and Woods, R.D. (1970), *Vibrations of Soils and Foundations*. Prentice Hall. Englewood Cliffs, NJ.
Sridharan, A., Gandhi, N.S.V.V.S.J. and Suresh, S. (1990), "Stiffness coefficients of layered soil systems", *J. Geotech. Eng. Div.*, ASCE, **116**(4), 604-624.
Whitman, R.V. and Richart, F.E., Jr. (1967), "Design procedures for dynamically loaded foundations", *J. Soil Mech. Found. Eng.,* ASCE, **93**(6), 169-193.

Nomenclature

A	: contact area of the footing
A_z	: displacement amplitude
Az_{max}	: maximum displacement amplitude
b	: mass ratio
B	: width of the model footing
D_r	: relative density
f_n	: natural frequency of the foundation-soil system
f_{nr}	: resonant frequency
f_{nf}	: natural frequency of finite sand stratum
f_{nh}	: natural frequency of homogeneous sand stratum
G	: shear modulus of homogeneous soil deposit
G_1	: shear modulus of finite sand stratum
G_2	: shear modulus of natural red-earth base
H	: thickness of the finite sand stratum
H/B	: height to width ratio

k_f : static stiffness of finite sand stratum
k_h : static stiffness homogeneous sand stratum
m : total mass of the vibrating system
m_e : eccentric mass provided in the oscillator
$m_e e$: force rating
r_o : equivalent radius of the model footing
ω : circular frequency of excitation
ω_n : circular natural frequency
ρ : mass density of the vibrating in-phase soil